Please cite this article as: Finnegan W., Meere M., Goggins J., 'The wave excitation forces on a truncated vertical cylinder in water of infinite depth'. Journal of Fluids and Structures 40(2013)201–213 (http://dx.doi.org/10.1016/j.jfluidstructs.2013.04.007)

The wave excitation forces on a truncated vertical cylinder in water of infinite depth

William Finnegan[1,3], Martin Meere[2], Jamie Goggins[1,3,*]

[1] *College of Engineering and Informatics, National University of Ireland, Galway, Ireland*

[2] *School of Mathematics, Statistics and Applied Mathematics, National University of Ireland, Galway, Ireland*

[3] *Ryan Institute for Environmental, Marine and Energy Research, National University of Ireland, Galway, Ireland*

** Tel: +35391492609, E-mail: jamie.goggins@nuigalway.ie*

Abstract

When carrying out any numerical modelling it is useful to have an analytical approximation available to provide a check on the accuracy of the numerical results and to give insight into the underlying physics of the system. The numerical modelling of wave energy converters is an efficient and inexpensive method of undertaking initial optimisation and experimentation. Therefore, the main objective of this paper is to determine an analytical approximation for the wave excitation forces on a floating truncated vertical cylinder in water of infinite depth. The approximation is developed by solving appropriate boundary value problems using the method of separation of variables. A graphical representation of the analytical approximation for the truncated vertical cylinder and the cylinder of infinite depth are presented and are compared to the results from a computational fluid dynamics analysis, using a commercial boundary element package. The presented analytical approximation and the computational fluid dynamics analysis results were found to be in good agreement. Furthermore, the presented analytical approximation was found to be in good agreement with independent experimental data.

Keywords: Analytical approximation; Excitation force; Infinite depth; Scattering problem; Floating truncated cylinder; Wave energy convertor.

Nomenclature

a radius of cylinder .... m

A amplitude of incident wave....................... m

A_s cross-sectional area .... m^2

b draft of cylinder.. m

C_m inertia coefficient ....

C_d drag coefficient..

F force.. N

F_c Fourier cosine transform ....

$F_{1,\text{ext}}$ surge excitation force............................... N

$F_{3,\text{ext}}$ heave excitation force............................... N

G gravity .... $m{\cdot}s^{-2}$

k_0 wavenumber .... m^{-1}

m integer ....

n_j j-component of the normal ....

$p_m(\xi)$ coefficient...

q_{m0} coefficient ....

$q_m(\xi)$ coefficient...

r radius.. m

S_B wetted surface...

t time.…………………………………………..s

T Location of pitch.………………………….

v flow velocity …………………………..... $m{\cdot}s^{-1}$

x horizontal coordinate .... m

z vertical coordinate .... m

ε_m Neumann symbol ....

θ polar coordinate.................................. rads

ξ separation constant ....

ρ *density* ..... $kg \cdot m^3$

φ *frequency domain velocity potential* ... $m \cdot s^{-1}$

φ_I *incident wave velocity potential* ..... $m \cdot s^{-1}$

φ_s^i *interior scattering velocity potential* ... $m \cdot s^{-1}$

φ_d^e *exterior diffraction velocity potential*.. $m \cdot s^{-1}$

φ_s^e *exterior scattering velocity potential*... $m \cdot s^{-1}$

Φ *time domain velocity potential* ..... $m \cdot s^{-1}$

χ^i *interior condensed function*.....

χ^e *exterior condensed function* .....

ω *wave angular frequency* ..... s^{-1}

1. Introduction

One of the main stages in the design of wave energy converters (WECs) is the numerical modelling of a given converter. In this paper, an analytical solution for the wave excitation forces on a floating truncated vertical cylinder in water of infinite depth is provided. This solution provides a method for validating the results of numerical models of WECs, since it estimates the forces on a cylinder representation of an arbitrary shaped axisymmetric WEC.

The solution of the scattering and radiation problem for floating bodies, in finite or infinite depth water, has being explored for decades for various shapes of bodies. Fritz Ursell (1949) explored the forces on an infinitely long horizontal floating cylinder in infinitely deep water using a polynomial set of stream functions to derive the analytical solution. Sir Thomas Havelock (1955) employed a similar technique to solve the radiation problem for a floating half-immersed sphere in infinitely deep water. MacCamy and Fuchs (1954) derived the analytical solution of a bottom mounted cylinder which penetrates the water surface in water of finite depth. Garrett (1971) formulated the solution for the scattering problem of oblique waves around a circular dock in water of finite depth and presented

numerical results detailing the vertical force, horizontal force and torque. Leppington (1973) examined the radiation properties of partially immersed three-dimensional bodies. A short-wave asymptotic limit was imposed in order to derive the velocity potential of the outgoing wave of a heaving and rolling circular dock and a heaving hemisphere. Bai (1975) developed a numerical method of linearizing the boundary value problem by using a variational principle equivalent in order to determine the diffraction of oblique waves by a horizontal infinitely long floating cylinder. This constructed variational form is employed by a finite element discretisation of the fluid domain and the numerical results are presented. Black (1975) investigated the wave forces on bodies which are vertically axisymmetric using an integral equation formulation in water of finite depth. Yeung (1981) presented a set of theoretical added mass and damping coefficients for a floating cylinder in water of finite depth and, also, truncated the solution for the infinite depth problem. Hsu and Wu (1997) developed a boundary element method to study the sway and heave motion of a 2-D floating rectangular structure in water of finite depth and an analytical solution for the problem was also presented. Mansour (2002) developed an analytical and boundary Integral Method (BIM) solution for a bottom-mounted uniform vertical cylinder with cosine-type radial perturbations which penetrates the water surface in water of finite depth and compared the numerical results to that of a circular cylinder. Bhatta and Rahman (2003) used the method of separation of variables technique, which is similar to that employed by Havelock (1955), to analyse the scattering and radiation problem for a floating vertical cylinder in water of finite depth and presented the formulation for the surge, heave and pitch motion solutions. Liu et al. (2012) developed an analytical solution using a matched eigenfunction expansion for the wave scattering by a submerged porous plate with finite thickness in water of finite depth and a boundary element method solution is also presented to confirm the analytical solution. Hassan and Bora (2012) employed the method of separation of variables to derive the exciting forces on a pair of coaxial hollow cylinder and bottom mounted cylinder in water of infinite depth and presented numerical results for a variety of radius to water depth ratios. Kang et al. (2012) proposed an analytical model for analysing the annular flow induced vibration of a simply supported cylinder, while also taking into account the effects of friction. Liu et al. (2012) used the multipole expansion method to obtain the analytical solution for the diffraction and radiation problem for a submerged

sphere in water of infinite depth and presented a set of numerical solutions for a variety of submerged depths. Similarly, Chatjigeorgiou (2012) employed the multipole expansion method in order to derive a solution for the hydrodynamic diffraction problem for a submerged oblate spheroid which is being excited by regular waves in deep water. Mohapatra et al. (2013) explored the effects of compressive flow on the wave diffraction on a 2-D floating elastic plate. The solution is derived for both the infinite and finite water depth cases using an integro-differential equation method.

However, an analytical study of the wave scattering problem of a floating truncated cylinder in water of infinite depth has not been previously attempted. Thus, in this paper, the method of separation of variables is employed to construct approximate analytical expressions for the wave excitation forces, by considering the wave scattering problem, on a floating truncated vertical cylinder in water of infinite depth. The results are compared with the output from a numerical computational fluid dynamics (CFD) analysis that was undertaken using the boundary element method package, ANSYS AQWA (2010). The presented analytical approximation is, also, compared to a curtailed version of the finite depth solution of Bhatta and Rahman (2003), where the water depth was set to a value which is considered deep, *200a*, in order to be comparable to the infinite depth approximation presented here. Furthermore, the presented approximation is compared with the experimental results given in Fonseca (2011).

2. Methodology

Since the desired solution deals with the scattering problem, the wave excitation forces on a fixed truncated vertical cylinder are considered with an incident wave of amplitude, A, and angular frequency, ω. A definition sketch depicting the set-up for the truncated vertical cylinder case is shown in **Fig. 1**. The wave progresses in the positive x-direction with $z = 0$ corresponding to the still water level (SWL) and the positive z-direction being taken to point directly down into the water. In this analysis, Linear (Airy) wave theory (Coastal Engineering Research Center, 1977) is used. Therefore, the following assumptions are made in the derivation of the governing mathematical model:

- The water is both incompressible, as frequencies are low, and effectively inviscid.
- As the air has such a small density relative to the water, pressure change is negligible and, thus, is at constant pressure.
- Surface tension at the air-water interface is negligible.
- The water is at constant density and temperature.
- The Reynolds number for the flow is sufficiently small for the flow to remain laminar.
- The waves are progressive and only travel in one direction and the wave motion is irrotational.
- The incident waves are of small amplitude compared to their wave length.

Following Yeung (1981) and Bhatta and Rahman (2003) the fluid domain was divided into an interior region and an exterior region. The interior region corresponds to the area underneath the cylinder and the exterior region constitutes the remainder of the domain (**Fig. 1**). The problem is solved in the frequency domain. Therefore, the time domain velocity potential, Φ, to be solved is transformed to the frequency domain, as follows:

$$\Phi(r,\theta,z,t) = Re\left[\varphi(r,\theta,z)\mathrm{e}^{-i\omega t}\right], \quad (1)$$

Where r is the radial distance from the z-axis, θ is the angle about the x-axis, i is the standard imaginary unit, ω is the wave angular frequency of the wave, t is time and φ is the frequency domain velocity potential. Applied forces to the cylinder are then calculated by integrating the relevant velocity potential over the wetted surface area of the cylinder, S_B, using the following equation(Linton and McIver, 2001):

$$\hat{F}_j = \mathrm{i}\rho\omega \iint_{S_B} \varphi\, n_j\, dS, \quad (2)$$

where ρ is water density, n_j is the j-component of the normal and $\hat{F}_j$ is defined implicitly by $F_j = Re\{\hat{F}_j \mathrm{e}^{-\mathrm{i}\omega t}\}$, where F_j is the force in the j-direction. The equations and boundary conditions, in cylindrical coordinates, that need to be satisfied are: Laplace's equation, the deep water condition, the free surface equation and the radiation condition, respectively (Linton and McIver, 2001):

$$\nabla^2\varphi = \frac{1}{r}\frac{\partial\varphi}{\partial r} + \frac{\partial^2\varphi}{\partial r^2} + \frac{1}{r^2}\frac{\partial^2\varphi}{\partial\theta^2} + \frac{\partial^2\varphi}{\partial z^2} = 0\,, \tag{3}$$

$$|\nabla\varphi| \to 0 \;\; as \;\; z \to \infty\,, \tag{4}$$

$$\omega^2\varphi + g\frac{\partial\varphi}{\partial z} = 0 \; on \; z = 0\,, r \geq a\,, \tag{5}$$

$$\lim_{r\to\infty}\sqrt{r}\left(\frac{\partial\varphi_d}{\partial r} - ik_0\varphi_d\right) = 0\,, \tag{6}$$

where ∇ is the gradient, g is the acceleration due to gravity, a is the radius of the cylinder, φ_d is the diffraction velocity potential and $k_0 = \omega^2/g$ is the wavenumber. Since the motion is irrotational and incompressible, Laplace's equation was arrived at by substituting $\boldsymbol{v} = \nabla\varphi$ into $\nabla.\boldsymbol{v} = 0$, where $\boldsymbol{v}$ is the flow velocity. The solution being developed is for infinitely deep water. Thus, the deep water condition defines the flow velocity near the sea bed. The free surface equation defines the velocity potential at the free surface away from the floating body. The radiation condition provides a constraint on the form of the velocity potential of the wave at distances from the body where the effect of the body on the wave has dissipated.

The velocity potential, φ, is a combination of the scattering velocity potential, φ_S, and the radiation velocity potential, φ_R, i.e. $\varphi = \varphi_S + \varphi_R$ (Linton and McIver, 2001). Since it is the excitation forces that is being sought and the radiation velocity potential determines the radiation forces on an oscillating body, only the scattering velocity potential needs to be derived. The truncated vertical cylinder problem considers a vertical cylinder of radius, a, and of draft, b, with an incident wave of amplitude, A, and angular frequency, ω, as depicted in **Fig. 1**. Since the scattering problem deals with the excitation force on a fixed body, the following structural boundary conditions must be imposed:

$$\frac{\partial\varphi_S^i}{\partial\bar{z}} = 0 \; on \; \bar{z} = 0\,, \qquad where \; \bar{z} = z - b\,, \tag{7}$$

$$\frac{\partial\varphi_S^e}{\partial r} = 0 \; at \; r = a\,, \qquad 0 < z < b\,, \tag{8}$$

where φ_S^i and φ_S^e are the interior and exterior scattering velocity potentials, respectively (see **Fig. 1**). The unknown coefficients are then determined by matching the interior and exterior scattering velocity potentials and their radial derivatives along their common boundary, $r = a$.

2.1 Derivation of velocity potential for the interior domain

The method of separation of variables is used to formulate an expression for the velocity potential. Since the problem deals with infinite depth, a Fourier sine/cosine transform is employed when dealing with the vertical or *z*-component. For the interior region, in order to satisfy the Neumann boundary condition on $\bar{z} = 0$ (**Eqn. (7)**), a Fourier cosine transform is required. Thus, the Fourier cosine transform of the interior scattering velocity potential, φ_S^i, is defined as follows:

$$F_c\left(\varphi_S^i(r,\theta,\bar{z})\right) = \sqrt{\frac{2}{\pi}}\int_0^\infty \varphi_S^i(r,\theta,\bar{z})\, cos\xi\bar{z}\, d\bar{z} \equiv \chi^i(r,\theta,\xi)\,, \tag{9}$$

where $0 < \xi < \infty$ and F_c is the Fourier cosine transform. The inverse transform is then:

$$\varphi_S^i(r,\theta,\bar{z}) = \sqrt{\frac{2}{\pi}}\int_0^\infty \chi^i(r,\theta,\xi)\, cos\xi\bar{z}\, d\xi\,. \tag{10}$$

The method of separation of variables is used to solve the Laplace's equation (**Eqn. (3)**) in order to formulate an expression for φ_S^i. Taking the Fourier cosine transform of each part of **Eqn. (3)** gives:

$$\frac{1}{r}\frac{\partial\chi^i}{\partial r} + \frac{\partial^2\chi^i}{\partial r^2} + \frac{1}{r^2}\frac{\partial^2\chi^i}{\partial\theta^2} - \xi^2\chi^i = 0\,. \tag{11}$$

Seeking separable variable solutions to **Eqn. (11)** of the form $\chi^i(r,\theta)$= *R(r)P(θ)* yields the following pair of ordinary differential equations:

$$r^2R'' + rR' - (\xi^2r^2 + \kappa)R = 0\,, \tag{12}$$

$$P'' + \kappa P = 0\,, \tag{13}$$

where κ is a separation constant. Solving **Eqn. (13)** and imposing 2π periodicity yields $\kappa = m^2$ and:

$$P_m(\theta) = A_m cosm\theta \quad for\ m = 0,1,2,3,\ldots \tag{14}$$

where the A_m are arbitrary constants. Solving **Eqn. (12)**, and imposing boundedness as $r \to 0$, gives:

$$R_m(r) = \begin{cases} B_{m0}r^m \ if\ \xi = 0 \\ B_m\mathrm{I}_m(\xi r)\ if\ \xi > 0 \end{cases}, \tag{15}$$

where the B_{m0} and B_m are arbitrary constants and I_m is the modified first Bessel function of order *m*. The separable variable solutions are thus:

$$\chi_m^i(r,\theta,\xi) = R_m(r)P_m(\theta) = \begin{cases} \frac{p_{m0}}{2}\left(\frac{r}{a}\right)^m \cos m\theta \;\; if\; \xi = 0 \\ p_m(\xi)\frac{\mathrm{I}_m(\xi r)}{\mathrm{I}_m(\xi a)}\cos m\theta \;\; if\; \xi > 0 \end{cases}, \qquad (16)$$

where $p_{m0} = a^m A_0 B_{m0}/2$ and $p_m(\xi) = A_m B_m \mathrm{I}_m(\xi a)$. Superposing these gives:

$$\chi_m^i(r,\theta,\xi) = \sum_{m=0}^{\infty}\left[\frac{p_{m0}}{2}\left(\frac{r}{a}\right)^m + p_m(\xi)\frac{I_m(\xi r)}{I_m(\xi a)}\right]\cos m\theta\,, \qquad r < a\,, \qquad (17)$$

and taking the inverse transform yields:

$$\varphi_S^i(r,\theta,\bar{z}) = \sum_{m=0}^{\infty}\left[\sqrt{\frac{2}{\pi}}\int_0^{\infty} p_m(\xi)\frac{\mathrm{I}_m(\xi r)}{\mathrm{I}_m(\xi a)}\cos\xi\bar{z}\; d\xi\right]\cos m\theta\,, \qquad r < a\,, \qquad (18)$$

where the choice $p_{m0} = 0$ has been made to remove a Dirac delta function from φ_S^i.

2.2 Derivation of velocity potential in the exterior domain

Next the exterior domain, $r > a$, is considered. The exterior scattering velocity potential is the sum of the incident and diffraction velocity potentials (i.e. $\varphi_S = \varphi_I + \varphi_d$). In this problem, a plane incident wave of amplitude, *A*, coming from $x = -\infty$ and propagating in the *x*-direction is considered, so that:

$$\varphi_I(r,\theta,z) = -\mathrm{i}\frac{gA}{\omega}\mathrm{e}^{-k_0 z}\mathrm{e}^{\mathrm{i}k_0 r\cos\theta}\,, \qquad (19)$$

since $x = r\cos\theta$. Kim (2008) has expanded this in the form:

$$\varphi_I(r,\theta,z) = -\frac{gA}{\omega}\mathrm{e}^{-k_0 z}\sum_{m=0}^{\infty}\epsilon_m \mathrm{i}^{m+1}\mathrm{J}_m(k_0 r)\cos m\theta\,, \qquad (20)$$

where J_m is a Bessel function of the first kind of order *m* and ε_m is the Neumann symbol, defined by $\varepsilon_0 = 1$ and $\varepsilon_m = 2$ for $m \geq 1$. Similar to the interior domain, when dealing with infinite depth in the method of separation of variables a Fourier sine/cosine transform is used. In order to satisfy the free surface equation (**Eqn. (5)**), a combination of the Fourier sine and Fourier cosine transform is

required. Thus, the Fourier cosine transform of the exterior diffraction velocity potential, $\varphi_{\mathrm{d}}^{\mathrm{e}}$, is defined as follows:

$$F\left(\varphi_{\mathrm{d}}^{\mathrm{e}}(r,\theta,z)\right) = \sqrt{\frac{2}{\pi}}\int_0^{\infty} \varphi_{\mathrm{d}}^{\mathrm{e}}(r,\theta,z)\,[\xi\cos\xi z - k_0\sin\xi z]dz = \chi^{e}(r,\theta,\xi)\,, \tag{21}$$

where $0 < \xi < \infty$. In order to obtain the inverse Fourier transform, Havelock's expansion theorem (Chakrabarti, 2000) is used, which states that if:

$$f(z) = C_0\mathrm{e}^{-Kz} + \sqrt{\frac{2}{\pi}}\int_0^{\infty} \frac{C(\xi)}{(\xi^2 + K^2)}[\xi\cos\xi z - K\sin\xi z]d\xi, \qquad 0 < \xi < \infty\,, \tag{22}$$

then

$$C_0 = 2K\int_0^{\infty} f(z)\mathrm{e}^{-Kz}\,dz\,, \tag{23}$$

$$C(\xi) = \sqrt{\frac{2}{\pi}}\int_0^{\infty} f(z)\,[\xi\cos\xi z - K\sin\xi z]dz\,, \tag{24}$$

where C_0 and K are constants and $f(z)$ and its derivatives are continuous and integrable in the range (0, ∞). Therefore, the inverse Fourier transform of **Eqn. (21)** is given as:

$$\varphi_d^e(r,\theta,z) = \chi_0(r,\theta)\mathrm{e}^{-k_0 z} + \sqrt{\frac{2}{\pi}}\int_0^{\infty} \frac{\chi^e(r,\theta,\xi)}{\xi^2 + {k_0}^2}[\xi\cos\xi z - k_0\sin\xi z]d\xi\,, \tag{25}$$

where

$$\chi_0(r,\theta) = 2k_0\int_0^{\infty} \varphi_d^e(r,\theta,z)\,\mathrm{e}^{-k_0 z}dz\,. \tag{26}$$

Now χ^e also satisfies **Eqn. (11)** and the variables are separated as before to obtain **Eqn. (14)**. Insisting that the solution remain bounded as $r \to \infty$, the following is then obtained:

$$R_m(r) = A_m \mathrm{K}_m(\xi r)\,, \tag{27}$$

where K_m is the modified second Bessel function of order *m*. Superposing the separated solutions gives:

$$\chi^e(r,\theta,\xi) = \sum_{m=0}^{\infty}\left[q_m(\xi)\frac{\mathrm{K}_m(\xi r)}{\mathrm{K}_m(\xi a)}\right]\cos m\theta\,, \qquad r > a\,. \tag{28}$$

In **Eqn. (25)**, $\chi_0(r,\theta)$ corresponds to ξ = -ik_0 and so the corresponding radial dependence is given by (Linton and McIver, 2001):

$$\mathrm{K}_m(\xi r) = \mathrm{K}_m(-\mathrm{i}k_0 r) = \frac{1}{2}\pi \mathrm{i}^{m+1}\mathrm{H}_m^{(1)}(k_0 r)\,, \tag{29}$$

where $\mathrm{H}_m^{(1)}$ is a Hankel function of the first kind of order *m*. Hence, the appropriate expansion for $\chi_0(r,\theta)$ is of the form:

$$\chi_0(r,\theta) = \sum_{m=0}^{\infty}\left[q_{m,0}\frac{\mathrm{H}_m^{(1)}(k_0 r)}{\mathrm{H}_m^{(1)}(k_0 a)}\right]\cos m\theta\,, \qquad r > a\,. \tag{30}$$

Therefore, since the scattering velocity potential is the sum of the incident and diffraction velocity potentials (i.e. $\varphi_S = \varphi_I + \varphi_d$) and incorporating -$gA\omega^{-1}\varepsilon_m \mathrm{i}^{m+1}$ into the $\varphi_d^e(r,\theta,z)$ term in **Eqn. (25)**, the scattering velocity potential for the exterior problem takes the form:

$$\varphi_S^e(r,\theta,z) = -\frac{gA}{\omega}\sum_{m=0}^{\infty}\epsilon_m \mathrm{i}^{m+1}\left[\left\{\mathrm{J}_m(k_0 r) + q_{m,0}\frac{\mathrm{H}_m^{(1)}(k_0 r)}{\mathrm{H}_m^{(1)}(k_0 a)}\right\}\mathrm{e}^{-k_0 z} + \sqrt{\frac{2}{\pi}}\int_0^{\infty}\frac{\mathrm{K}_m(\xi r)}{\mathrm{K}_m(\xi a)}\frac{q_m(\xi)}{\xi^2 + {k_0}^2}[\xi\cos\xi z - k_0\sin\xi z]d\xi\right]\cos m\theta\,. \tag{31}$$

2.3 Determination of unknown coefficients

The unknown coefficients of $p_m(\xi)$ in **Eqn. (18)**, and $q_{m,0}$ and $q_m(\xi)$ in **Eqn. (31)**, are found by matching the velocity potentials and normal velocities across the boundary at $r = a$, and imposing the structural boundary condition. The conditions which are to be satisfied at the boundary are:

$$\left.\frac{\partial \varphi_S^e(r,\theta,z)}{\partial r}\right|_{r=a} = 0\,, \qquad if\ 0 \le z \le b\,, \tag{32}$$

$$\varphi_S^e(r,\theta,z)|_{r=a} = \left.\varphi_S^i(r,\theta,\bar{z})\right|_{r=a}\,, \qquad if\ b \le z \le \infty\,, \tag{33}$$

$$\left.\frac{\partial \varphi_S^e(r,\theta,z)}{\partial r}\right|_{r=a} = \left.\frac{\partial \varphi_S^i(r,\theta,\bar{z})}{\partial r}\right|_{r=a}\,, \qquad if\ b \le z \le \infty\,. \tag{34}$$

Leppington (1973) derives the velocity potential along the free-surface in the outer region, as the majority of the velocity potential of significant magnitude is at the free-surface for high-frequency waves. Leppington (1973) then expands from to derive the full field outer velocity potential. In dealing with the inner region, a rescaling of coordinates is performed so a solid body (i.e. a dock) having a semi-infinite extent is being solved for. A similar technique is employed in this paper in approximating the exterior scattering velocity potential, as the majority of this potential with significant magnitude is close the free-surface in the region $0 < z < b$. Since the presented study is not restricted to high-frequency waves, this assumption is deemed valid by ensuring that the draft to radius ratio remains greater than unity, i.e. $b/a > 1$, throughout the analysis.

In order to derive an analytical approximation for the interior and exterior velocity potentials, the following procedure is adopted. Closed form expressions for $q_{m,0}$ and $q_m(\xi)$ (and consequently φ_S^e) are constructed by taking $b = \infty$ in the boundary condition, given in **Eqn. (32)**, which corresponds to calculating the exterior scattering velocity potential for a cylinder of infinite draft. The matching condition, given in Eqn. (33), is then imposed to determine $p_m(\xi)$ and φ_S^i. Finally, the surge and heave excitation forces are then found using the calculated forms for φ_S^e and φ_S^i, respectively. The justification for this approach lies in the comparison with corresponding numerical CFD results. The parameter space for the problem under consideration here is two dimensional and may be represented by the region $0 < k_0a,\ b/a < \infty$ in the (k_0a, b/a) plane. Extensive CFD work conducted for the current

study indicates the analytical expressions for the surge and heave forces derived are acceptable provided the non-dimensional parameters (k_0a, b/a) lie in the region $0 < k_0a < \infty$, $1 < b/a < \infty$.

The procedure just described is now implemented. In the exterior region, the condition which is to be satisfied is given in **Eqn. (32)**, where $b = \infty$, and is then applied to **Eqn. (31)**, yielding:

$$-\frac{gA}{\omega}\epsilon_m \mathrm{i}^{m+1} k_0 \left\{ \mathrm{J}_m{}'(k_0a) + q_{m,0} \frac{\mathrm{H}_m^{(1)}{}'(k_0a)}{\mathrm{H}_m^{(1)}(k_0a)} \right\} \mathrm{e}^{-k_0 z}$$

$$-\frac{gA}{\omega}\epsilon_m \mathrm{i}^{m+1} \sqrt{\frac{2}{\pi}} \int_0^\infty \frac{\xi \mathrm{K}_m{}'(\xi a)}{\mathrm{K}_m(\xi a)} \frac{q_m(\xi)}{\left(\mu^2 + {k_0}^2\right)} [\xi \cos \xi z \tag{35}$$

$$- k_0 \sin \xi z] d\xi = 0 ,$$

which is then rearranged to give

$$k_0 q_{m,0} \frac{\mathrm{H}_m^{(1)}{}'(k_0a)}{\mathrm{H}_m^{(1)}(k_0a)} \mathrm{e}^{-k_0 z} + \sqrt{\frac{2}{\pi}} \int_0^\infty \frac{\xi \mathrm{K}_m{}'(\xi a)}{\mathrm{K}_m(\xi a)} \frac{q_m(\xi)}{\left(\mu^2 + {k_0}^2\right)} [\xi \cos \xi z - k_0 \sin \xi z] d\xi \tag{36}$$

$$= -k_0 \mathrm{J}_m^{'}(k_0a) \mathrm{e}^{-k_0 z} ,$$

where the prime is the derivative. Havelock's expansion theorem (Chakrabarti, 2000) is then applied to **Eqn. (36)** in order to determine the unknown coefficients. Therefore,

$$q_{m,0} \frac{\mathrm{H}_m^{(1)}{}'(k_0a)}{\mathrm{H}_m^{(1)}(k_0a)} = -2k_0 \int_0^\infty \mathrm{J}_m{}'(k_0a) \mathrm{e}^{-k_0 z} \mathrm{e}^{-k_0 z} \, dz$$

$$= -2k_0 \mathrm{J}_m^{'}(k_0a) \frac{1}{2k_0} [\mathrm{e}^{-2k_0 z}]_0^\infty = -\mathrm{J}_m{}'(k_0a) , \tag{37}$$

and

$$q_m(\xi) = \sqrt{\frac{\pi}{2}} \frac{2}{\pi\left(\xi^2 + {k_0}^2\right)} \int_0^\infty \mathrm{J}_m{}'(k_0a) \mathrm{e}^{-k_0 z} [\xi \cos \xi z - k_0 \sin \xi z] dz$$

$$= \sqrt{\frac{2}{\pi}} \frac{\mathrm{J}_m{}'(k_0a)}{\xi^2 + {k_0}^2} \left[\xi \frac{k_0}{\xi^2 + {k_0}^2} - k_0 \frac{\xi}{\xi^2 + {k_0}^2} \right] = 0 . \tag{38}$$

Next, using this result, taking **Eqn. (18)** and **Eqn. (31)** and the condition in **Eqn. (33)** yields:

$$\sqrt{\frac{2}{\pi}}\int_b^\infty p_m(\xi)\cos\xi(\mathrm{z}-\mathrm{b})\,d\xi = -\frac{gA}{\omega}\epsilon_m \mathrm{i}^{m+1}\{\mathrm{J}_m(k_0a)+q_{m,0}\}\mathrm{e}^{-k_0z}\,. \tag{39}$$

Therefore, inverting the Fourier cosine transform gives:

$$p_m(\xi) = \sqrt{\frac{2}{\pi}}\int_b^\infty \left\{-\frac{gA}{\omega}\epsilon_m \mathrm{i}^{m+1}\{\mathrm{J}_m(k_0a)+q_{m,0}\}\mathrm{e}^{-k_0z}\right\}\cos\xi(\mathrm{z}-\mathrm{b})\,dz = -\frac{gA}{\omega}\epsilon_m \mathrm{i}^{m+1}\sqrt{\frac{2}{\pi}}\left\{\mathrm{J}_m(k_0a)-\mathrm{J}_m{}'(k_0a)\frac{\mathrm{H}_m^{(1)}(k_0a)}{\mathrm{H}_m^{(1)}{}'(k_0a)}\right\}\frac{\mathrm{e}^{-k_0b}k_0}{\xi^2+{k_0}^2}\,. \tag{40}$$

Consequently, the interior scattering velocity potential, given in **Eqn. (18)**, is written as:

$$\varphi_{\mathrm{S}}^{\mathrm{i}}(r,\theta,\bar{\mathrm{z}}) = -\frac{gA}{\omega}\frac{2}{\pi}\sum_{m=0}^{\infty}\left[\epsilon_m \mathrm{i}^{m+1}\left\{\mathrm{J}_m(k_0a)-\mathrm{J}_m'(k_0a)\frac{\mathrm{H}_m^{(1)}(k_0a)}{\mathrm{H}_m^{(1)}{}'(k_0a)}\right\}\int_0^\infty \frac{\mathrm{e}^{-k_0b}k_0}{\xi^2+{k_0}^2}\frac{\mathrm{I}_m(\xi r)}{\mathrm{I}_m(\xi a)}\cos\xi\bar{\mathrm{z}}\;d\xi\right]\cos m\theta\;, \tag{41}$$

and the exterior scattering velocity potential, given in **Eqn. (31)**, is written as:

$$\varphi_S^e(r,\theta,z) = -\frac{gA}{\omega}\sum_{m=0}^{\infty}\epsilon_m \mathrm{i}^{m+1}\left[\left\{\mathrm{J}_m(k_0r)-\mathrm{J}_m'(k_0a)\frac{\mathrm{H}_m^{(1)}(k_0r)}{\mathrm{H}_m^{(1)}{}'(k_0a)}\right\}\mathrm{e}^{-k_0z}\right]\cos m\theta\,. \tag{42}$$

In this section, the scattering velocity potentials for the exterior region, $r > a$, and interior region, $r < a$, were formulated and the unknown coefficients were approximated by matching these velocity potentials at $r = a$. Therefore, for the truncated cylinder case, the interior scattering velocity potential (**Eqn. (41)**) and the exterior scattering velocity potential (**Eqn. (42)**) are now approximated.

3. Results

In this section, the wave excitation forces for both the truncated and infinite draft cylinder cases are derived using the relevant velocity potentials and **Eqn. (2)**. The three motions from which the wave excitation forces are been calculated for the truncated cylinder case are the surge, heave and pitch. Since, for the infinite draft cylinder case, there is no vertical, or heave motion, only the surge excitation force is calculated. These solutions are presented for a range of frequencies and, for the truncated cylinder case, for a range of draft to radius ratios also. In order to verify the accuracy of the analytical solution, the wave excitation forces are compared to the output from a numerical computational fluid dynamics (CFD) analysis that was undertaken using the boundary element method package, ANSYS AQWA (2010). Since the numerical CFD analysis uses a finite depth solution, it is necessary to set the water depth in the model to *1000m*, in order to be comparable to the presented infinite depth analytical approximation.

3.1 Wave excitation forces on a truncated cylinder

When calculating the surge, or horizontal, excitation force the only non-zero contribution is for $m = 1$, as this gives the only non-zero value amongst the integral $\int_0^{2\pi} cosm\theta\ cos\theta\ d\theta$, which arise in the force calculation. Furthermore, when integrating the velocity potential over the surface area, the integration is performed only over the curved surface of the cylinder and, hence, the exterior velocity potential at the surface boundary, $r = a$, given in **Eqn. (42)**, is used. Therefore, the surge excitation force, $\hat{F}_{1,\text{ext}}$, is given as:

$$\hat{F}_{1,\text{ext}} = \mathrm{i}\rho\omega \iint_{S_B} \varphi_S^e(r,\theta,z)\, n_1\, dS = -\mathrm{i}\rho\omega \int_0^{2\pi}\int_0^b \varphi_S^e(a,\theta,z)\cos\theta\; a\; dz\; d\theta$$

$$= -\frac{\rho g A a}{k_0}\sum_{m=0}^{\infty} \varepsilon_m\, \mathrm{i}^m \left\{ \mathrm{J}_m(k_0 a) - \mathrm{J}_m{}'(k_0 a)\frac{\mathrm{H}_m^{(1)}(k_0 a)}{\mathrm{H}_m^{(1)}{}'(k_0 a)} \right\} \Big(1$$

$$- \mathrm{e}^{-k_0 b}\Big) \int_0^{2\pi} \cos m\theta \cos\theta \; d\theta \qquad (43)$$

$$= -\frac{2\pi \mathrm{i}\rho g A a}{k_0} \left\{ \mathrm{J}_1(k_0 a) - \mathrm{J}_1{}'(k_0 a)\frac{\mathrm{H}_1^{(1)}(k_0 a)}{\mathrm{H}_1^{(1)}{}'(k_0 a)} \right\} \left(1 - \mathrm{e}^{-k_0 b}\right),$$

where n_1 = -cos θ. Graphical representations of surge excitation forces with respect to incident wave frequencies for various draft to radius ratios of truncated vertical cylinders are shown in **Fig. 2**. As can been seen, the presented analytical solution and the numerical CFD solution are in good agreement even for quite modest draft to radius ratios. The correspondence between the analytical and numerical CFD solutions improves as the draft to radius ratio increases as would be expected, since the exterior velocity potential is derived assuming that the cylinder in question has infinite draft. The shaded region on the graph indicates where all the possible choices of draft to radius ratio which will return a valid solution. The upper bound is calculated where the draft is set to infinity and the lower bound is where the draft is set to zero, for a very thin plate, in the presented approximation for the surge excitation force, given in **Eqn. (43)**. Furthermore, the phase angle of the excitation forces as $k_0 a$ varies is shown in **Fig. 3**, where the phase angle, β, is defined in the equation:

$$F(t) = \left|\hat{F}\right| \cos(\omega t + \beta), \qquad (44)$$

where $\hat{F}$ is the relevant excitation force. As can be seen from **Fig. 3**, there is good agreement between the analytical solutions and the numerical CFD solutions for the phase angle over a range of frequency waves (i.e. $k_0 a$).

When calculating the heave, or vertical, excitation force from the velocity potential, the only non-zero value is for $m = 0$ since this gives the only non-vanishing term in the integral $\int_0^{2\pi} cosm\theta\; d\theta$. Furthermore, when integrating the velocity potential over the surface area, the integration is

performed only over the base of the cylinder and, hence, the interior velocity potential, at $\bar{z}= 0$, given in **Eqn. (41)**, is used. Therefore, the heave excitation force, $\hat{F}_{3,\text{ext}}$, is given as:

$$\hat{F}_{3,\text{ext}} = \mathrm{i}\rho\omega \iint_{S_B} \varphi_S^i(r,\theta,\bar{z})\, n_3\, dS = \mathrm{i}\rho\omega \int_0^{2\pi}\int_0^a \varphi_S^i(r,\theta,0) n_3 r\, dr\, d\theta$$

$$= -\mathrm{i}\rho\omega \sqrt{\frac{2}{\pi}} \sum_{m=0}^{\infty} \int_0^{2\pi}\int_0^a \int_0^{\infty} p_m(\xi) \frac{\mathrm{I}_m(\xi r)}{\mathrm{I}_m(\xi a)}\, d\xi\, r\, dr \cos m\theta\, d\theta \quad (45)$$

$$= -2\pi\mathrm{i}\rho\omega a \sqrt{\frac{2}{\pi}} \int_0^{\infty} p_0(\xi) \frac{\mathrm{I}_1(\xi a)}{\xi \mathrm{I}_0(\xi a)}\, d\xi\,,$$

where $n_3 = -1$. Graphical representations of heave excitation forces with respect to incident wave frequencies for various draft to radius ratios of truncated vertical cylinders are shown in **Fig. 4** and the phase angle of the heave excitation forces is shown in **Fig. 3**.Again, in **Fig. 4**, as with **Fig. 2**, the agreement between the presented analytical solution and the numerical CFD solutions is good and improves as the draft to radius ratio increases. However, in **Fig. 4**, the upper bound for the normalised heave is calculated where the draft is set to zero, for a very thin plate, and the lower bound is where the draft is set to infinity in the presented approximation, given in **Eqn. (45)**. This is to be expected as the water particle velocity decreases exponentially from the still water level downwards and, therefore, the vertical force on the base will, in turn, decrease as the draft to radius ratio increases.

The pitch, or torque, excitation force arises from the surge and heave forces on the wetted surface of the cylinder. The pitch is taken about the axis which is transverse to the incident wave at the centre of the base, as shown by *T* in **Fig. 1**. When calculating the pitch the only non-zero contribution, similar to surge, is from $m = 1$. Therefore, the pitch excitation force, $\hat{F}_{5,\text{ext}}$, is given as:

$$\hat{F}_{5,\text{ext}} = \mathrm{i}\rho\omega \iint_{S_B} \varphi_S(r,\theta,z)\, n_5 \, dS$$

$$= \mathrm{i}\rho\omega \int_0^{2\pi} \int_0^b \varphi_S^e(a,\theta,z)(z-b)\cos\theta \; a \; dz \; d\theta$$

$$- \mathrm{i}\rho\omega \int_0^{2\pi} \int_0^a \varphi_S^i(r,\theta,0) r^2 \cos\theta \; dr \; d\theta \qquad (46)$$

$$= -2\pi\mathrm{i}\rho g A a \left\{ \mathrm{J}_1(k_0 a) - \mathrm{J}_1'(k_0 a) \frac{\mathrm{H}_1^{(1)}(k_0 a)}{\mathrm{H}_1^{(1)\prime}(k_0 a)} \right\} \frac{1 - k_0 b - \mathrm{e}^{-k_0 b}}{{k_0}^2}$$

$$+ \pi\mathrm{i}\rho\omega a^2 \sqrt{\frac{2}{\pi}} \int_0^\infty p_1(\xi) \frac{\mathrm{I}_2(\xi a)}{\xi \mathrm{I}_1(\xi a)} \, d\xi \, ,$$

where $n_5 = (z - b)\, n_1 - r \cos\theta \, n_3$. Graphical representations of the analytical pitch excitation forces with respect to incident wave frequencies for various draft-radius ratios of truncated vertical cylinders are shown in **Fig. 5**. The trends of **Fig. 5** are very similar to that of **Fig. 2** as the magnitude of the pitch increases as the draft of the cylinder increases and the lower bound is where the draft is zero, for a very thin plate. However, since it is pitch that is being calculated and that is proportional to the draft an upper limit for the problem cannot be calculated. This is to be expected in view of the choice of axis about which the pitch is taken. It is also noted that the phase angle of the pitch excitation forces is the same as that for the surge excitation forces, as shown in **Fig. 3**, and this was also observed by Garrett (1971) for the finite depth case.

The analytical approximation presented in this paper is compared to a curtailed version of the finite depth solution of Bhatta and Rahman (2003) in **Fig. 6** and **7** for the normalised surge and heave excitation forces, respectively. In order to ensure the two sets of results are comparable, the water depth was set to a value which is considered deep, *200a*, in the finite depth solution of Bhatta and Rahman (2003). The results from the corresponding numerical CFD analysis are also included in **Fig. 6** and **7**. It is clear to see from this comparison that the numerical model and analytical approximation yield similar trends of normalised force varying with frequency waves ($k_o a$). As the draft to radius ratio increases, the two sets of results are found to be in very good agreement. Furthermore, it may be

noted that the presented analytical approximation converges quicker to the numerical CFD than the finite depth solution from Bhatta and Rahman (2003) in the case of the surge wave excitation force calculation.

Using physical models, Fonseca (2011) estimated the first order wave excitation forces on a truncated vertical cylinder with a radius, *a = 0.325m*, and a draft, *b = 0.2m*. Since the experimental results are being compared to an infinite depth approximation, only the regular wave observations for a water depth of *3m* are used in the comparison and are displayed in **Fig. 8**. This independently observed experimental data is compared to the presented solution for a truncated vertical cylinder with a draft to radius ratio, *b/a = 0.62*. From **Fig. 8**, it can be seen that the presented analytical expressions are in good agreement with the experimental data.

3.2 Wave excitation forces on a cylinder of infinite depth

The scattering velocity potential, φ_S, was derived in **Section 2.3** for a cylinder of infinite draft yielding the solution given in **Eqn. (42)**. On the other hand, for a bottom mounted cylinder in water of finite depth, *d*, and using a concurrent axis orientation as that presented in this paper, MacCamy and Fuchs (1954) obtained the solution:

$$\varphi_S(r,\theta,z) = -\frac{gA}{\omega}\frac{\cosh k_0(d-z)}{\cosh k_0 d}\sum_{m=0}^{\infty}\epsilon_m \mathrm{i}^{m+1}\left\{\mathrm{J}_m(k_0 r) - \mathrm{J}_m'(k_0 a)\frac{\mathrm{H}_m^{(1)}(k_0 r)}{\mathrm{H}_m^{(1)}'(k_0 a)}\right\}\cos m\theta\,, \tag{47}$$

for a bottom mounted cylinder in water of finite depth, *d*. For the infinite depth case, the z-component of the equation is replaced with $\mathrm{e}^{-k_0 z}$. Thus, the solution presented in **Eqn. (42)** corresponds with the infinite depth version of MacCamy and Fuchs (1954) solution given in **Eqn. (47)**. The surge excitation force, in the frequency domain, $\hat{F}_{1,\mathrm{ext}}$, is then calculated as follows:

$$\hat{F}_{1,\text{ext}} = \mathrm{i}\rho\omega \iint_{S_B} \varphi_S(r,\theta,z)\, n_1\, dS = \mathrm{i}\rho\omega \int_0^{2\pi}\int_0^{\infty} \varphi_S(a,\theta,z) n_1 a\, dz\, d\theta$$

$$= -\frac{\rho g A a}{k_0} \sum_{m=0}^{\infty} \epsilon_m \mathrm{i}^m \left[\mathrm{J}_m(k_0 a) - \mathrm{J}_m'(k_0 a) \frac{\mathrm{H}_m^{(1)}(k_0 a)}{\mathrm{H}_m^{(1)\prime}(k_0 a)} \right] \int_0^{2\pi} \cos m\theta \cos\theta\, d\theta \tag{48}$$

$$= -\frac{2\pi \mathrm{i}\rho g A a}{k_0} \left[\mathrm{J}_1(k_0 a) - \mathrm{J}_1'(k_0 a) \frac{\mathrm{H}_1^{(1)}(k_0 a)}{\mathrm{H}_1^{(1)\prime}(k_0 a)} \right],$$

where n_1 = - cos θ and the only non-zero solution to $\int_0^{2\pi} \cos m\theta \cos\theta \; d\theta$ is when $m = 1$. Since the exterior velocity potential is calculated for the exterior domain, the solution is the same as when $b = \infty$ in **Eqn. (43)**. In **Fig. 9**, the presented solution is also compared to a numerical CFD solution, performed using the BEM software ANSYS AQWA (2010). Since the draft of the cylinder cannot be set to infinity in the numerical CFD solution, a draft to radius ratio, *b/a = 20*, is used. This comparison of the two solutions is found to be in good agreement except at low frequencies. This difference is as a result of the parameter, *b/a = 20*, in the numerical CFD solution and greater values for the draft to radius ratio would yield closer agreement. When this parameter is applied to the analytical solution, i.e. *b/a = 20*, the two solutions match up very well as can be seen in **Fig. 9**.

4. Discussion and Conclusions

An analytical approximation to determine the wave excitation forces, by solving the scattering problem, on a floating truncated vertical cylinder in water of infinite depth has been presented in this paper. The presented analytical approximation provides a solution which is far easier to use and implement than the already available analytical solutions. For example, the solution for the finite depth case provided by Bhatta and Rahman (2003) requires a considerable amount of further work if numerical values for a particular case are needed. On the other hand, the formulation presented in this paper yields an easy to implement analytical approximation for the surge, heave and pitch wave

excitation forces on a truncated cylinder. This was achieved by imposing an approximation in deriving the unknown coefficients in the exterior region. Furthermore, the presented analytical approximation still retains a high level of accuracy in calculating the heave and surge wave excitation forces, when the draft to radius ratio is greater than unity.

The method of separation of variables is employed in order to formulate the velocity potentials and the unknown coefficients are derived by matching these potentials along their common boundaries. In order to create an analytical solution, the exterior velocity potential is derived for the case of a vertical cylinder of infinite draft and the interior velocity potential is calculated by matching across their common boundary. However, it should be noted that this assumption is a good approximation when the draft to radius ratio is greater than or equal to unity (i.e. $b/a \geq 1$), which can been seen in **Fig. 2, 4 and 5**, where the presented analytical solution and numerical CFD solution are in increasingly better agreement as the draft to radius ratio (b/a) increases.

The relationships between wave excitation forces and wave frequency ($k_o a$) are shown graphically in **Fig. 2, 4 and 5** for a truncated cylinder having various draft to radius ratios. It may be noted that the pitch excitation forces are also derived in the study, along with the heave and surge excitation forces. These results are validated by comparing to a numerical CFD solution, performed using the BEM software ANSYS AQWA (2010), and they are found to be in very good agreement. A shaded region on the graph is also included indicating where a viable solution may be obtained. For surge and pitch motions, the upper bound is calculated where the draft is infinite and the lower bound is where the draft is zero, for a very thin plate. However, for heave motion, the upper bound of the viable solution region is calculated where the draft is zero, for a very thin plate, and the lower bound is where the draft is infinite. This is to be expected as the water particle velocity decreases exponentially from the still water level downwards and, therefore, the vertical force on the base will, in turn, decrease as the draft to radius ratio increases. These three figures (**Fig. 2, 4, 5)** and the associated approximations provide an efficient and relatively quick solution to the problem for an engineer or professional investigating the wave excitation forces on a floating structure in deep water.

The phase angles of the wave excitation forces, relative to the incident wave, are also presented graphically in **Fig. 3** and compared to the results from a numerical CFD analysis. The presented

analytical results were found to be in good agreement with the results from the numerical CFD analysis. Furthermore, when compared to the independently observed experimental data given in Fonseca (2011), the analytical solution for a truncated vertical cylinder shows good agreement, as shown in **Fig. 8**.

In addition, the presented analytical approximation is compared to a curtailed version of the finite depth solution of Bhatta and Rahman (2003), which is shown graphically for the normalised surge and heave excitation forces in **Fig. 6** and **Fig. 7,** respectively. It is clear from this comparison that similar trends occur with respect to the relation between the normalised excitation forces and frequency waves (i.e. k_0a) for the presented analytical approximation and a curtailed version of the finite depth solution of Bhatta and Rahman (2003), as with the numerical CFD results. As the draft to radius ratio increases, the two sets of results are found to be in very good agreement.

Furthermore, when deriving the exterior velocity potential it was found to match to the infinite depth version of the MacCamy and Fuchs equation (MacCamy and Fuchs, 1954). In addition, the presented solution, for the infinite draft cylinder case, is also compared to a numerical CFD solution and they are found to be in very good agreement, which can be seen in **Fig. 9**.

The analytical solution provided in this paper provides an engineer with a very good approximation of the wave excitation forces on a structure which may be represented by a truncated cylinder. Furthermore, if only the k_0a value is known, the maximum forces can easily be calculated from the analytical solution, or estimated from the shaded regions of the graphs in **Fig. 2, 4, 5**, to aid in the design stage of an offshore structure.

Acknowledgements

The first author would like to acknowledge the financial support from the National University of Ireland under the College of Engineering & Informatics Postgraduate Fellowship. The authors would also like to express their gratitude to the anonymous reviewers of this paper for their constructive comments.

References

ANSYS-Inc., ANSYS AQWA, Release 13. 2010.

Bai K.J., 1975. Diffraction of oblique waves by an infinite cylinder. Journal of Fluid Mechanics. 68(03): p. 513-535.

Bhatta D.D., Rahman M., 2003. On scattering and radiation problem for a cylinder in water of finite depth. International Journal of Engineering Science. 41(9): p. 931-967.

Black J.L., 1975. Wave forces on vertical axisymmetric bodies. Journal of Fluid Mechanics. 67(02): p. 369-376.

Chakrabarti A., 2000. On the Solution of the Problem of Scattering of Surface-Water Waves by the Edge of an Ice Cover. Proceedings: Mathematical, Physical and Engineering Sciences. 456(1997): p. 1087-1099.

Chatjigeorgiou I.K., 2012. Hydrodynamic exciting forces on a submerged oblate spheroid in regular waves. Computers & Fluids. 57(0): p. 151-162.

Coastal Engineering Research Center, 1977. Shore protection manual / U.S. Army Coastal Engineering Research Center. Fort Belvoir, Va. Washington: Supt. of Docs., U.S. Govt. Print. Off.

Finnegan W., Meere M., Goggins J., The Wave Excitation Forces on a Floating Vertical Cylinder in Water of Infinite Depth, in World Renewable Energy Congress 2011. 2011: Linkoping Sweden.

Fonseca N., Pessoa J.o., Mavrakos S., Le Boulluec M., 2011. Experimental and numerical investigation of the slowly varying wave exciting drift forces on a restrained body in bi-chromatic waves. Ocean Engineering. 38(17-18): p. 2000-2014.

Garrett C.J.R., 1971. Wave forces on a circular dock. Journal of Fluid Mechanics. 46(01): p. 129-139.

Hassan M., Bora S.N., 2012. Exciting forces for a pair of coaxial hollow cylinder and bottom-mounted cylinder in water of finite depth. Ocean Engineering. 50(0): p. 38-43.

Havelock T., 1955. Waves due to a Floating Sphere Making Periodic Heaving Oscillations. Proceedings of the Royal Society of London. Series A, Mathematical and Physical Sciences. 231(1184): p. 1-7.

Hsu H.-H., Wu Y.-C., 1997. The hydrodynamic coefficients for an oscillating rectangular structure on a free surface with sidewall. Ocean Engineering. 24(2): p. 177-199.

Kang H.S., Mureithi N.W., Pettigrew M.J., 2012. Analytical solution for a vibrating simply-supported cylinder subjected to 2-D concentric annular flow, considering friction. Journal of Fluids and Structures. 35(0): p. 1-20.

Kim C.H., 2008. Nonlinear Waves and Offshore Structures. Advanced Series on Ocean Engineering: World Scientific Publishing Co. Pte. Ltd.

Leppington F.G., 1973. On the radiation and scattering of short surface waves. Part 3. Journal of Fluid Mechanics. 59(01): p. 147-157.

Linton C.M., McIver P., 2001. Handbook of Mathematical Techniques for Wave/Structure Interactions. Boca Raton, FL: Chapman & Hall/CRC.

Liu Y.-y., Teng B., Cong P.-w., Liu C.-f., Gou Y., 2012. Analytical study of wave diffraction and radiation by a submerged sphere in infinite water depth. Ocean Engineering. 51(0): p. 129-141.

Liu Y., Li H.-J., Li Y.-C., 2012. A new analytical solution for wave scattering by a submerged horizontal porous plate with finite thickness. Ocean Engineering. 42(0): p. 83-92.

MacCamy R.C., Fuchs R.A., Wave Forces on Piles: A Diffraction Theory, in Tech. Memo No. 69. 1954, US Army Corps of Engineers, Beach Erosion Board.

Mansour A.M., Williams A.N., Wang K.H., 2002. The diffraction of linear waves by a uniform vertical cylinder with cosine-type radial perturbations. Ocean Engineering. 29(3): p. 239-259.

Mohapatra S.C., Ghoshal R., Sahoo T., 2013. Effect of compression on wave diffraction by a floating elastic plate. Journal of Fluids and Structures. 36(0): p. 124-135.

Ursell F., 1949. On the heaving motion of a circular cylinder on the surface of a fluid The Quarterly Journal of Mechanics and Applied Mathematics. 2(2): p. 218-231.

Yeung R.W., 1981. Added mass and damping of a vertical cylinder in finite-depth waters. Applied Ocean Research. 3(3): p. 119-133.

Figure Captions

Fig. 1 Definition sketch for the boundary value problem for a truncated vertical cylinder (Finnegan et al., 2011)

Fig. 2 The normalised surge (or horizontal) excitation force, in the frequency domain, as a function of k_0a, for various draft-radius ratios compared to the corresponding numerical CFD analysis

Fig. 3 The phase angle for surge and heave, in the frequency domain, as a function of k_0a, compared to the corresponding numerical CFD analysis

Fig. 4 The normalised heave (or vertical) excitation force, in the frequency domain, as a function of k_0a, for various draft-radius ratios compared to the corresponding numerical CFD analysis

Fig. 5 The normalised pitch (or torque) excitation force, in the frequency domain, as a function of k_0a, for various draft-radius ratios

Fig. 6 The normalised surge (or horizontal) excitation force, in the frequency domain, as a function of k_0a, for various draft-radius ratios compared to Bhatta and Rahman (2003) and to the corresponding numerical CFD analysis

Fig. 7 The normalised heave (or vertical) excitation force, in the frequency domain, as a function of k_0a, for various draft-radius ratios compared to Bhatta and Rahman (2003) and to the corresponding numerical CFD analysis

Fig. 8 Comparison of the normalised heave and surge wave excitation forces with the experimental results of Fonseca (2011)

Fig. 9 Dependence of normalised surge excitation force on k_0a and compared to the corresponding numerical CFD analysis

Figure

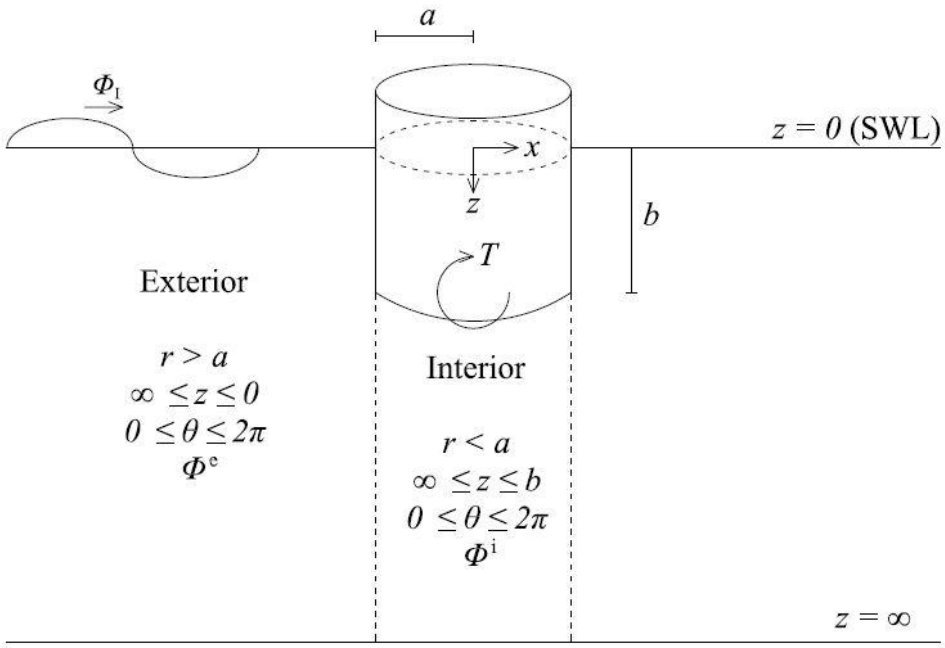

Fig. 1 Definition sketch for the boundary value problem for a truncated vertical cylinder (Finnegan et al., 2011)

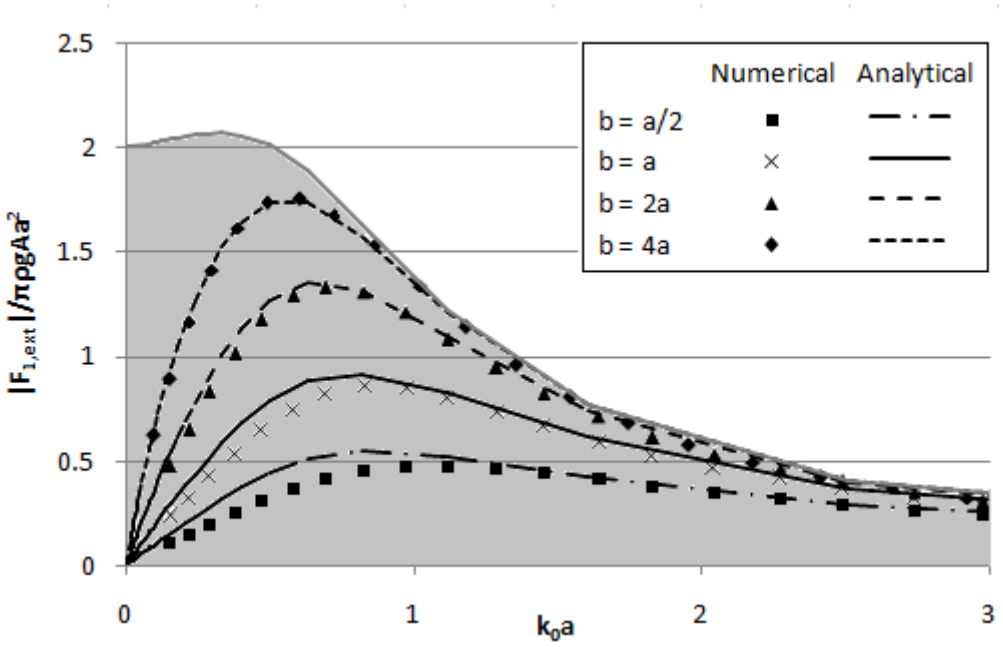

Fig. 2 The normalised surge (or horizontal) excitation force, in the frequency domain, as a function of $k_0 a$, for various draft-radius ratios compared to the corresponding numerical CFD analysis

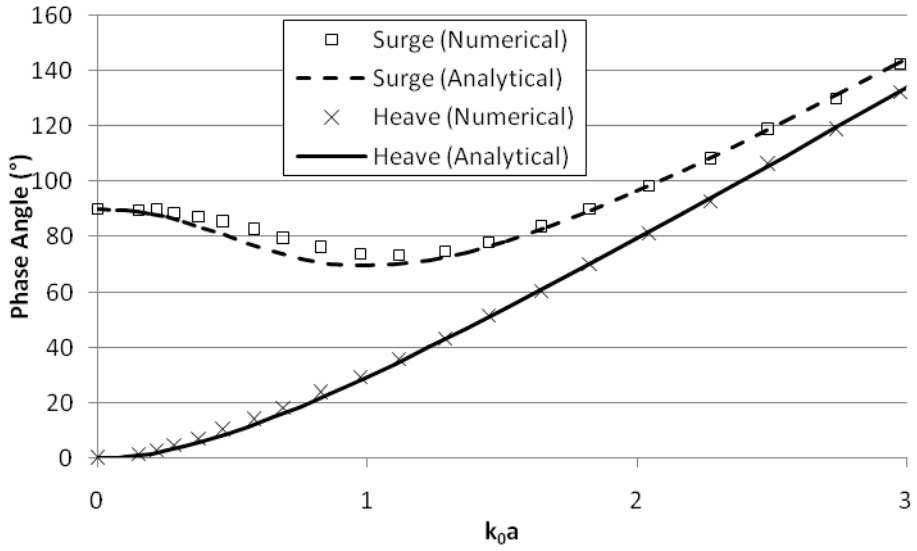

Fig. 3 The phase angle for surge and heave, in the frequency domain, as a function of k_0a, compared to the corresponding numerical CFD analysis

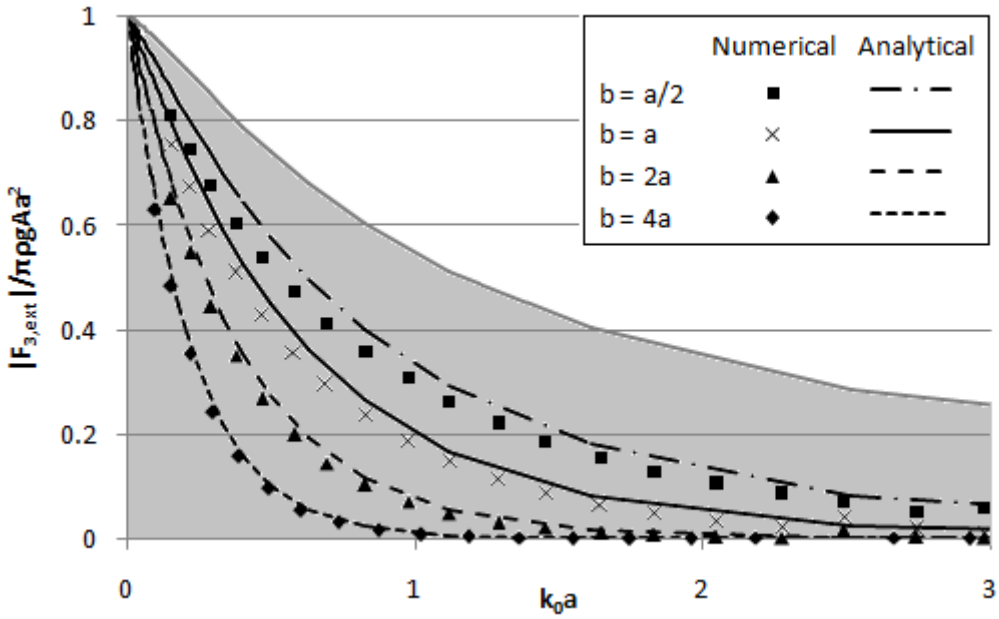

Fig. 4 The normalised heave (or vertical) excitation force, in the frequency domain, as a function of k_0a, for various draft-radius ratios compared to the corresponding numerical CFD analysis

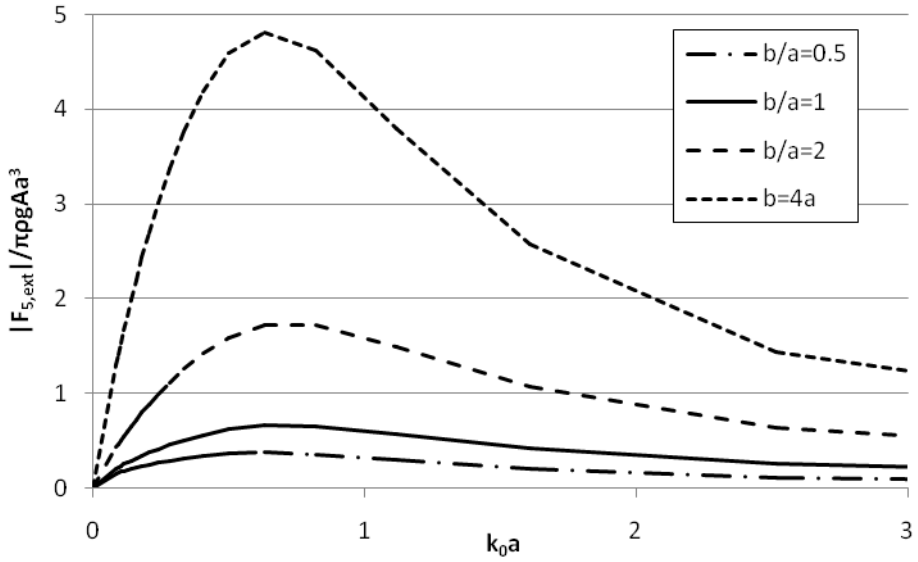

Fig. 5 The normalised pitch (or torque) excitation force, in the frequency domain, as a function of k_0a, for various draft-radius ratios

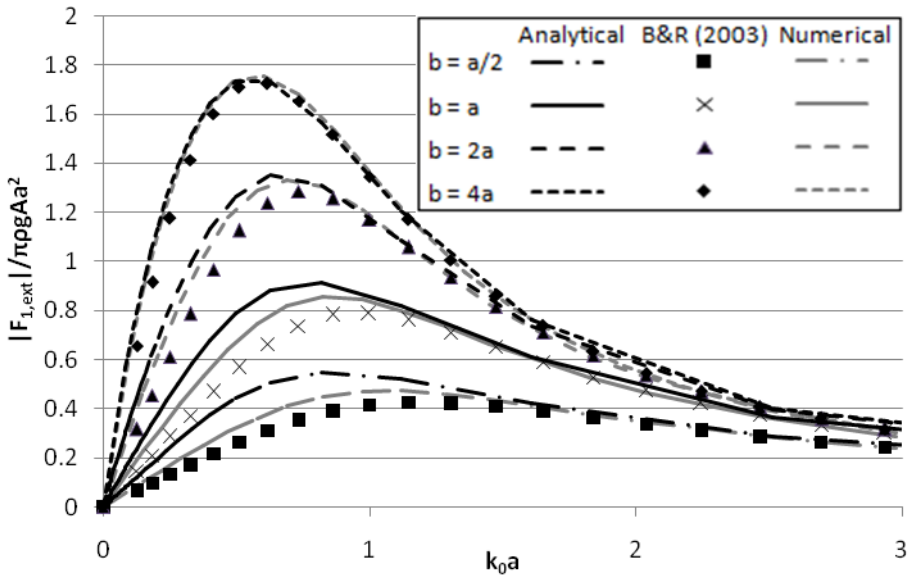

Fig. 6 The normalised surge (or horizontal) excitation force, in the frequency domain, as a function of k_0a, for various draft-radius ratios compared to Bhatta and Rahman (2003) and to the corresponding numerical CFD analysis

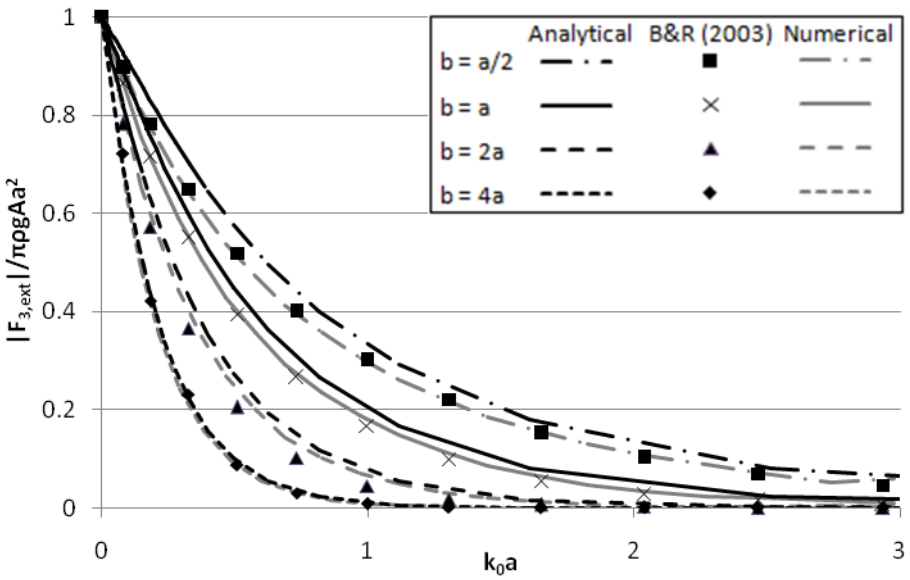

Fig. 7 The normalised heave (or vertical) excitation force, in the frequency domain, as a function of k_0a, for various draft-radius ratios compared to Bhatta and Rahman (2003) and to the corresponding numerical CFD analysis.

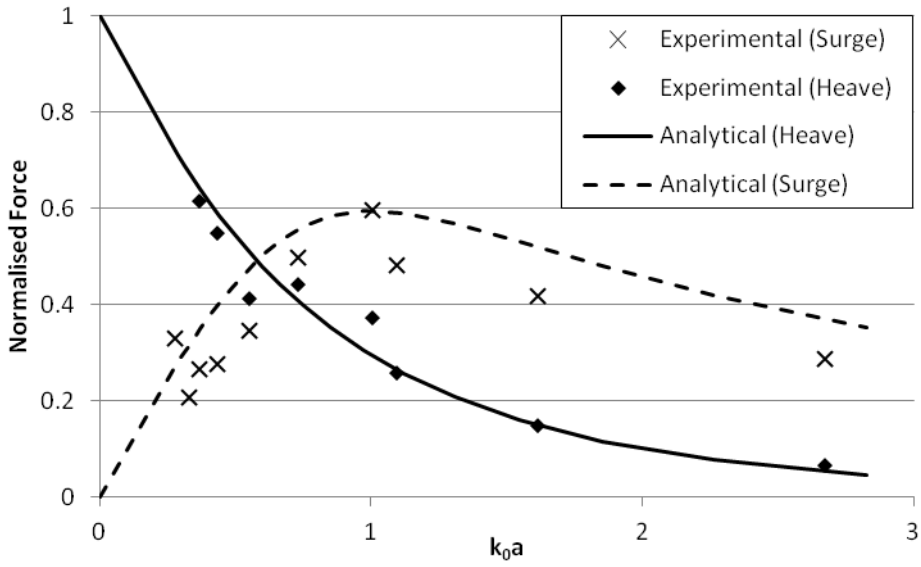

Fig. 8 Comparison of the normalised heave and surge wave excitation forces with the experimental results of Fonseca (2011)

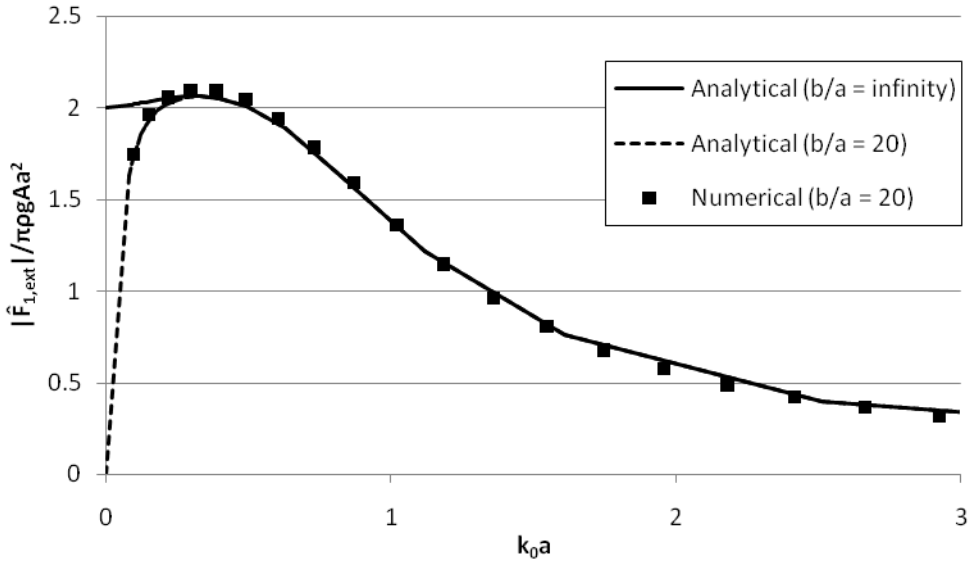

Fig. 9 Dependence of normalised surge excitation force on k_0a and compared to the corresponding numerical CFD analysis